Model to Predict Treatment Response to Trastuzumab in HER2 Positive Metastatic Gastric Cancer Patients

Dongwoo Chae

Department of Medical Science

The Graduate School, Yonsei University

Model to Predict Treatment Response to Trastuzumab in HER2 Positive Metastatic Gastric Cancer Patients

Directed by Professor Kyung Soo Park

The Doctoral Dissertation

submitted to the Department of Medical Science,

the Graduate School of Yonsei University

in partial fulfillment of the requirements for the degree of

Doctor of Philosophy

Dongwoo Chae

December 2016

This certifies that the Doctoral Dissertation of Dongwoo Chae is approved

---

Thesis Supervisor: Kyung Soo Park

Thesis Committee Member #1: Hyun Chul Chung

Thesis Committee Member #2: Chung Mo Nam

Thesis Committee Member #3: Sun Young Rha

Thesis Committee Member #4: Jae Ho Chung

The Graduate School

Yonsei University

December 2016

ACKNOWLEDGEMENTS

연구자로써, 그리고 한 인간으로써 성장할 수 있도록 도와주신 박경수 교수님께 진심으로 감사를 드립니다. 본 학위 논문의 자문위원으로 많은 도움을 주신 정현철, 남정모, 라선영, 정재호 교수님께 감사를 드립니다. 훌륭한 연구 기관으로써 약리학 교실을 발전 시켜주신 김경환 교수님, 안영수 교수님, 김동구 교수님, 이민구 교수님, 김철훈 교수님, 김주영 교수님, 김형범 교수님, 지헌영 교수님께 진심으로 감사 드립니다. 늘 저희를 챙겨주시는 임종수 선생님, 김건태 선생님, 민선자 선생님께도 깊은 감사를 드립니다.

가까운 곳에서 응원해 준 저희 연구실 대학원생 모두에게 고마운 마음을 전하며 연구를 하면서 어려운 점을 같이 상의할 수 있었던 친구이자 동기인 이정호에게도 고마움의 마음을 전합니다. 마지막으로 아버지, 어머니께 사랑한다고 말씀 드리고 싶습니다. 이 모든 주변 분들의 도움이 없었다면 저는 결코 무사히 연구를 해나갈 수 없었을 것입니다.

2016 년 12 월 채동우

TABLE OF CONTENTS

ABSTRACT 1

I. INTRODUCTION 3

II. MATERIALS AND METHODS 5

1. Theory development 5

A. Models of Tumor Growth and Progression 5

(A) Density dependence 5

(B) Tumor progression 6

B. Models of Chemotherapy Response 7

(A) Dose-response curves 7

(B) K-PD model 9

C. Time to Event Models 11

(A) Progression Free Survival and Overall Survival 11

(B) Hazard functions 11

(C) Covariate incorporation into the hazard function 13

2. Data 14

3. Exploratory Data Analysis 19

4. MODELS 20

A. Tumor Size Model 20

B. Covariate Model 25

C. Survival Model 25

D. Model Evaluation 26

III. RESULTS 28

1. Exploratory Data Analysis 28

A. Baseline tumor size, Ksh, and DoR 28

B. Distribution of DoR 36

2. Tumor Size Model 38

3. Survival Model 41

A. PFS prediction model 41

B. PPS prediction model 42

4. Model Evaluation 43

A. Goodness of fit plots of the tumor size model 43

B. Validation 44

1. Data 49

2. Tumor size model (Model 1) 49

3. Survival Model 50

A. PFS prediction model 50

B. PPS prediction model 50

V. CONCLUSION 51

REFERENCES 52

ABSTRACT (IN KOREAN) 59

LIST OF FIGURES

Figure 1. Maximum Tumor Diameter [mm] vs. Time [months]. 17

Figure 2. Kaplan Meier Curves of Progression Free (left) and Overall (right) Survival. 18

Figure 3. Diagram of treatment response model. 23

Figure 4. A typical tumor curve under treatment. 24

Figure 5. Baseline tumor size [mm] vs. early tumor shrinkage rate [/mo] 28

Figure 6. Depth of response (DoR) vs. Early shrinkage rate. 29

Figure 7. Predicted DoR vs. Ksh in HER2 3+ and 0/1+/2+ patients. 30

Figure 8. PFS as a function of DoR. 31

Figure 9. Histogram with kernel density estimates of DoR overlaid. 36

Figure 10. K-means clustering of (Ksh, DoR). 37

Figure 11. Pruned decision tree diagram to predict DoR class. 38

Figure 12. Distribution of post-hoc trastuzumab resistance probability. 40

Figure 13. Distribution of post-hoc 5-FU resistance (=cisplatin

resistance) probability. 41
Figure 14. Mirror plots of the tumor size model. 43
Figure 15. Basic goodness of fit plots of the tumor size model. 44
Figure 16. VPC of the tumor size model using the index dataset (n=1,000). 45
Figure 17. VPC of the tumor size model using the validation dataset (n=1,000). 45
Figure 18. Simulated (red) and observed (blue) KM survival curves of PFS using training data (n=1,000). 46
Figure 19. Validation of PFS prediction using test data (n=1,000) 46
Figure 20. Simulated (red) and observed (blue) KM survival curves of PPS using training data (n=1,000). 47
Figure 21. Validation of PPS prediction using test data (n=1,000). 47

LIST OF TABLES

Table 1. Patient demographics and covariates of training and test datasets 15

Table 2. Significant covariates affecting PFS using observed DoR 33

Table 3. Significant covariates affecting PFS using predicted DoR using observed Ksh 34

Table 4. Metastatic status and baseline tumor size 34

Table 5. Response rate (RR), depth of response (DOR) and PFS stratified by trastuzumab treatment and HER2 receptor status 35

Table 6. Estimation result of tumor size model 38

Table 7. Estimation results of Model 2 42

Table 8. Estimation results of PPS prediction model 42

ABSTRACT

Model to Predict Treatment Response to Trastuzumab in HER2 Positive Metastatic Gastric Cancer Patients

Dongwoo Chae

Department of Medical Science

The Graduate School, Yonsei University

(Directed by Professor Kyung Soo Park)

Objectives

This study was carried out to build a comprehensive mathematical model to predict treatment outcome in HER2 positive metastatic gastric cancer patients.

Materials and Methods

Data were collected from 69 advanced gastric cancer patients who participated in a clinical study conducted in Severance hospital, Seoul, Korea, as part of ToGA clinical trial. Sum of longest diameter of target lesions was evaluated at each clinic visit based on RECIST criteria. A tumor growth inhibition (TGI) model was developed under a K-PD modeling framework. Parametric survival models were

subsequently built to link TGI model predictions to PFS and PPS. A separate dataset consisting of 86 patients was used for model validation.

Results

The tumor size predictions generated by the developed TGI model provided a good fit with the observed tumor sizes. HER2 3+ patients showed higher sensitivity to trastuzumab compared to HER2 1+/2+ patients. Higher WHO histologic grades were associated with faster tumor progression. Prior gastrectomy history and lower ECOG score were associated with lower hazard of non-measurable lesion PD. PFS and PPS showed positive correlation when WHO histologic grade were either I or II. Such correlation disappeared for WHO histologic grades of III and IV.

Conclusion

Based on the developed model, it is possible to generate individualized predictions of treatment response and patient survival. This will help optimize treatment in HER2 positive metastatic gastric cancer patients.

Model to Predict Treatment Response to Trastuzumab in HER2 Positive Metastatic Gastric Cancer Patients

Dongwoo Chae

Department of Medical Science

The Graduate School, Yonsei University

(Directed by Professor Kyung Soo Park)

I. INTRODUCTION

In 2010, FDA granted approval for trastuzumab in combination with cisplatin and a fluoropyrimidine for the treatment of patients with HER2 overexpressing metastatic gastric or gastroesophageal (GE) junction adenocarcinoma. The approval was based on a significant improvement in median overall survival of 2.5 mos with trastuzumab plus chemotherapy treatment compared to chemotherapy alone demonstrated in the ToGA clinical trial.[1] Subsequent research found that trastuzumab treatment prolonged survival of HER2 positive patients significantly more than HER2 negative patients. [2]

Currently, a standardized dosing regimen of trastuzumab with initial loading dose of 8 mg/kg followed by a maintenance dose of 6 mg/kg every 3 wks is used to treat all HER2 positive metastatic gastric cancer patients. Clearly, there is no consideration of factors such as tumor burden, histology, or HER2 status. In an era of personalized

medicine, unfavorable consequences of ignoring individual variability are being increasingly acknowledged.

To achieve optimal individualized therapy, one must first acquire individual predictions of treatment response. Precise predictions often need computerized system built upon validated mathematical models.

Based on known physiology and landmark discoveries made in the past few decades,[3-10] we have sought to build a physiological model of tumor size dynamics and rely on computer simulations to investigate the complex nature of treatment responses.

Such an approach is gaining increasing popularity in recent years. There is now a rich library of published tumor growth inhibition (TGI) models proposed by numerous research groups. [11-15]

The greatest benefit of using computational models to estimate dose-response relationship stems from its comprehensive nature. Once tumor size changes can be predicted, various endpoints can be automatically deduced. For example, intermediate endpoints such as early tumor shrinkage (ETS) and depth of response (DoR),[16-22] can be easily deduced from the tumor size dynamics. Progressive disease (PD), as defined in RECIST [23] criteria, can also be predicted by calculating the time at which the predicted tumor size rises above 20% of the minimum.

In this work, we have successfully developed a tumor growth inhibition (TGI) model of metastatic gastric cancer patients and linked it with patient survival. Our model system would enable the clinicians to predict treatment responses in patients harboring different covariates.

Theoretical exposition on tumor growth and chemotherapy response will be given first.

II. MATERIALS AND METHODS

1. Theory development

A. Models of Tumor Growth and Progression

The fundamental property of any proliferating cell is the doubling time (DT), defined as the time needed for doubling of its volume. Specific growth rate (SGR; %/time) is defined as log(2)/DT.[24]

A general equation describing tumor growth is shown below:

$$\frac{dN}{dt} = k_g(N,t)N \qquad \cdots \qquad (1.1.1)$$

N denotes tumor size and $k_g(N,t)$ specific growth rate.

(A) Density dependence

Due to scarcity of resources, tumor growth often slows down as tumor size gets larger. Logistic and Gompertz models are widely used to describe such behavior.

$$k_g(N,t) = r_g\left(1 - \frac{N}{N_{max}}\right) \qquad \text{(Logistic growth model)}$$

$$k_g(N,t) = r_g \log\left(\frac{N_{max}}{N}\right) \qquad \text{(Gompertz growth model)}$$

Dependence of specific growth rate (k_g) on N is defined as 'density dependence' of tumor growth.

(B) Tumor progression

It is being increasingly recognized that genotypes (and phenotypes) of cancer cells in an individual are highly heterogeneous.[25,26] Such heterogeneity is primarily generated through random mutations and is the driving force of clonal evolution.[27]

The following equation is known in evolutionary game theory as the 'replicator equation'[28].

$$\frac{dx_k}{dt} = (f_k(x) - k_g(x))x_k \qquad \dots \qquad (1.1.2)$$

In the above, x_k is the proportion of type k in the population, x = (x_1, …, x_n) is the vector of the distribution of types in the population, $f_k(x)$ is the fitness of type k, and $k_g(x)$ is the average population fitness.

The fitness $f_k(x)$ in our work is defined as the specific growth rate of type k. $k_g(x)$ is then the average SGR of the population x.

Based on Eq. (1.1.2), the following can be derived.

$$\frac{dk_g(x)}{dt} = \sum(f_k(x) - k_g(x))^2 x_k \qquad \dots \qquad (1.1.3)$$

Since the elements of the population vector x sum to unity by definition, the (R.H.S.) of Eq. (1.1.3) can be interpreted as the variance of $f_k(x)$ defined on the support vector x. This important conclusion is known as 'Fisher's fundamental theorem of natural selection'[8].

We will denote $\frac{dk_g(x)}{dt}$ (= $\sum(f_k(x) - k_g(x))^2 x_k$) as β in our work. As we shall see, β is one of the most important parameters of our model.

B. Models of Chemotherapy Response

(A) Dose-response curves

The log-kill hypothesis of chemotherapy (first established by Skipper and colleagues [29,30]) in the 1960s found that in experimental tumors, cell-kill increased logarithmically with dose.

Denoting S as the surviving cell fraction,

$$S = \exp(-kD) \qquad \dots (1.2.1)$$

(D: total dose, k: rate constant of cell kill)

Since total dose is proportional to AUC, Eq. (1.2.1) can also be expressed as:

$$S = \exp(-kAUC) \qquad \dots (1.2.2)$$

For many cell cycle phase-specific drugs, cytotoxicity is not a simple function of AUC. Time of exposure may be more important than drug concentration, and plateaus in cytotoxicity are observed with increasing drug concentrations. Adams [31] proposed that appropriate weighting must incorporating into either concentration or time. That is,

$$S=\exp(-k\int C^n\, dt) \qquad \dots (1.2.3)$$

Larger n would result in more weight given to drug concentration. In the extreme case of n=0, drug concentration has no role to play and it is the exposure time alone that determines response.

In addition to drug response being a complex function of both drug exposure and treatment time, it was soon discovered that treatment response is often dependent on tumor size itself.

In 1988, Norton fit a Gompertzian model to human breast cancer growth.[32] Under the Gompertzian model, the tumor growth rate attenuates with tumor age and size, implying that smaller tumors are relatively more susceptible to chemotherapy. Using this as theoretical motivation, Norton and Simon proposed the "Norton-Simon hypothesis", which was stated as follows:

"Therapy results in a rate of regression in tumor volume that is proportional to the rate of growth that would be expected for an unperturbed tumor of that size."

In mathematical terms, unperturbed tumor growth is described as follows:

$$\frac{dN}{dt} = k_g N \log \frac{N_{max}}{N} \quad \ldots (1.2.4)$$

In the presence of chemotherapy, Eq. (1.2.4) changes to:

$$\frac{dN}{dt} = (k_g - k_{eff}) N \log \frac{N_{max}}{N} \quad \ldots (1.2.5)$$

Here, k_{eff} is a coefficient of drug efficacy. If log-kill hypothesis were true, the equation should have been:

$$\frac{dN}{dt} = k_g N \log \frac{N_{max}}{N} - k_{eff} N \quad \ldots (1.2.6)$$

It has been found in many cases that Eq. (1.2.5) is a closer description of reality than Eq. (1.2.6). From a mathematical perspective, log-kill hypothesis and Norton Simon hypothesis are corollaries of exponential and Gomperz-type growth models, respectively, associated with negative specific growth rates.

(B) K-PD model

It is often the case that plasma concentration information is absent. In these circumstances, a way to use dose information as a substitute has been proposed in the classic papers.[33,34]

The simplest approach is to use dose as a simple covariate. With this assumption, Eq. (1.2.3) becomes:

$$S=\exp(-k\int Dose^{n}\,dt) \qquad (1.2.7)$$

Problem with this approach is that dose is assumed to distribute evenly within each dosing interval.

To mimic the entry and elimination of drug into and out of the biophase, a hypothetical compartment might be introduced. Jacqmin[34] named this hypothetical compartment as 'virtual' compartment. Note that virtual compartment does not correspond to any real physiological entity.

In the original formulation by Jacqmin, a single virtual compartment receives bolus input of the drug. The drug is eliminated from this virtual compartment at a rate proportional to the amount in the compartment (i.e. 1st order elimination). The author, however, states that the input profile for the virtual PK compartment can be more complex, including for example zero or first order input rates, if the PD data allows the identification of the extra input parameters [34].

A K-PD model with a single delay compartment can be modeled as shown below:

$\frac{dC}{dt}$ = -KDE· C (delay compartment)

$\frac{dV}{dt}$ = KDE· (C − V) (virtual compartment)

After bolus input into compartment C, the drug is transferred to V with a rate constant KDE.

KDE·V then acts as an exposure measure which is fed into one of the following functions:

Drug effect = k_{eff} KDE·V (Linear model)

Drug effect = k_{eff} log(1 + KDE·V) (Log-linear model)

Drug effect = $\frac{E_{max}\text{KDE}\cdot V}{EC_{50}+\text{KDE}\cdot V}$ (Ordinary Emax model)

Drug effect = $\frac{E_{max}(\text{KDE}\cdot V)^{\gamma}}{EC_{50}{}^{\gamma}+(\text{KDE}\cdot V)^{\gamma}}$ (Sigmoid Emax model)

In our work, we have used the K-PD modeling framework to incorporate dose information of trastuzumab, cisplatin, and capecitabine/5-FU.

C. Time to Event Models

(A) Progression Free Survival and Overall Survival

Progression Free Survival (PFS) is the time to progressive disease (PD).

According to the revised RECIST guideline (version 1.1)[23], progressive disease (PD) can be diagnosed based on measurable lesions defined as the sum of longest diameters of target lesions or non-measurable lesions that include leptomeningeal disease, ascites, pleural or pericardial effusion, inflammatory breast disease, lymphangitic involvement of skin or lung, abdominal masses/abdominal organomegaly identified by physical exam that is not measurable by reproducible imaging techniques. Because of the contribution of non-measurable lesions, we need a separate model other than a tumor size prediction model to predict PD.

Overall survival (OS) is the time to patient death.

Both PFS and OS are calculated relative to the reference time point of baseline assessment at the beginning of study.

(B) Hazard functions

If in a unit time interval the hazard of an event is h, the number of events would be hN(t), where N(t) denotes the maximum number of events at a given time t.

Survival S(t) is defined as N(t)/N(0). It is the ratio of maximum number of occurrence at time t to that at time 0.

Since at each time the number of events is hN(t), the rate of change of N(t) is -hN(t). The negative sign denotes that once an event occurs for a certain individual, that individual is excluded from subsequent analysis.

From $\frac{dN(t)}{dt}$ = -hN(t), separating variables and integrating yields N(t) = N(0)exp(-ht). Hence, survival S(t) = N(t)/N(0) = exp(-ht). Assuming constant hazard, survival is simply an exponential function. Otherwise, h(t) is often assumed to follow a certain distribution. Commonly used probability distributions to describe time varying hazard are (1) Weibull, (2) Gompertz-Makeham, (3) gamma, (4) generalized gamma, (5) log-normal, (6) log-logistic, and many others.[35]

Weibull model assumes that hazard is propotional to a certain power of time.

$$h(t) = h^p p t^{p-1}$$

When p = 1, the Weibull model reduces to a constant hazard model since dependence on time is eliminated. If p > 1, the hazard will increase monotonically with time. If 0 < p < 1, the hazard will decrease monotonically with time.

A similar model is Gompertz-Makeham model:

$$h(t) = \exp(a + bt)$$

It is often the case that hazard function is hump-shaped (i.e. there is a time window of maximal hazard after which the hazard decreases again). Log-normal hazard model is simply a log-normal distribution having time as the independent variable.

A log-logistic model is defined as shown below:

$$h(t) = \frac{h^p p t^{p-1}}{1+(ht)^p}$$

Log-logistic hazard has a characteristic hump shape and is appropriate for modeling hazards that increases and then decreases.

(C) Covariate incorporation into the hazard function

The hazard function can be affected by different covariates. The most widely used method to incorporate covariates is a generalized linear model using a logarithmic transformation.

$$\text{Log(h)} = \beta_0 + \beta_1 cov_1 + \ldots + \beta_n cov_n$$

This is called a proportional (or multiplicative) hazard model.

Less often, hazard is formulated as a simple linear combination of the covariates.

$$\text{h} = \beta_0 + \beta_1 cov_1 + \ldots + \beta_n cov_n$$

This is called an additive hazard model. Unlike proportional hazard model, the absolute change in risk, instead of the risk ratio, is of primary interest. A recent article that used additive hazard regression model to analyze the natural history of human papillomavirus [36] should serve as a good reference.

2. Data

A total of 69 advanced gastric cancer patients enrolled into ToGA phase III clinical trial who received either of the following regimens - Trastuzumab + XP/FP or XP/FP – as 1st line therapy, beginning from December 2005 in Severance hospital, Seoul, Korea, were used for model building.

ToGA trial is a multi-centered trial to evaluate the efficacy of Trastuzumab in HER2 overexpressing gastric and GEJ cancer patients. Patients whose gastric or GEJ tumors showed HER2 overexpression by IHC or gene amplification by FISH were eligible for the study. Patients were randomized in equal numbers to capecitabine 1000 mg/m^2/day on days 1-14 followed by 1 week rest (or 5-FU 800 mg/m^2/day on days 1-5 continuous infusion), cisplatin 80 mg/m^2/day on day 1 every 3 weeks for six cycles or to capecitabine (or 5-FU), cisplatin and trastuzumab 8 mg/kg loading dose on day 1 followed by 6 mg/kg every 3 weeks.[1] Trastuzumab was continued until progression of the disease.

In the published article [1], it was shown that OS was improved significantly with the addition of trastuzumab (13.8 mos in trastuzumab arm compared with 11.1 mos in the chemotherapy alone arm, p = 0.0046). Median PFS was 6.7 mos in the trastuzumab arm compared to 5.5 months in the chemotherapy alone arm (p = 0.0002). The overall response rate was 47.3% versus 34.5% in trastuzumab plus chemotherapy and chemotherapy, respectively (p = 0.0017).

Post hoc exploratory analysis showed that trastuzumab and chemotherapy improved OS in patients with IHC 2+ and FISH positive or IHC 3+ patients compared with IHC 0 or 1+ and FISH-positive patients.

In our analysis dataset, RECIST evaluation was done at every clinic visit (which took place approximately every 3 wks) and maximum tumor diameter (mm) was

recorded. Time of PD diagnosis and patient death were also recorded, and progression free survival and overall survival calculated. Extra information regarding the cause of PD (tumor growth > 20% relative to best response, appearance of new lesion, or clinical deterioration) was also given.

In addition to basic patient demographics, histologic grade, organs of metastases, and ECOG score were also recorded. The summary of analysis datasets is shown in Table 1.

Table 1. Patient demographics and covariates of training and test datasets

Characteristics	**Training dataset (n=69)**	**Test dataset (n=86)**	**P-value**
Age [yrs] (median, range)	59 (33-80)	60 (36-82)	0.78†
Gender	Male: 47 Female: 22	Male: 63 Female: 23	0.60‡‡
Weight [kg] (mean ± sd)	59.06 ± 9.58	61.87 ± 10.32	0.081†
Baseline tumor size [mm] (median, range)	73.60 (10.40-429.00)	42.25 (1.10-252.80)	0.0001††
Histologic grade			
Well	7 (10.14%)	5 (5.68%)	
Moderate	40 (57.97%)	42(47.72%)	
Poor	18 (26.09%)	36 (40.91%)	0.14‡
Signet ring cell	4 (5.80%)	4(4.55%)	
Mucinous	0 (0.00%)	1 (1.14%)	
HER2 receptor status			

Negative	5 (7.25%)	19 (22.09%)	0.021‡‡
Positive	64 (92.75%)	67 (77.91%)	
ECOG score			
0	32 (46.38%)	54 (62.79%)	0.12‡
1	29 (42.03%)	27 (31.40%)	
2-3	8 (11.59%)	5 (5.81%)	
Previous gastrectomy	52 (75.36%)	26 (30.23%)	<0.0001‡‡
Metastatic status			
Liver	32 (25.81%)	44 (25.88%)	
Peritoneum	22 (17.74%)	37 (21.76%)	
Distant lymph nodes	50 (40.32%)	57 (33.53%)	0.49‡
Ovary	5 (4.03%)	3 (1.76%)	
Brain	0 (0.00%)	1 (0.59%)	
Lung	9 (7.26%)	21 (12.35%)	
Bone	6 (4.84%)	7 (4.12%)	
Lauren classification			
Intestinal	15 (21.74%)	17 (19.77%)	
Diffuse	3 (4.35%)	5 (5.81%)	0.96‡
Mixed	1 (1.45%)	1 (1.16%)	
Unknown	50 (72.46%)	63 (73.26%)	
Progression free survival [days] (median, range)	218 (14-1440)	215 (30-1987)	0.56†
Overall survival [days] (median, range)	428 (76-2423)	254 (30-1987)	0.16†

The raw data plots of tumor size vs. time and survival are shown in Figure 1 and 2, respectively.

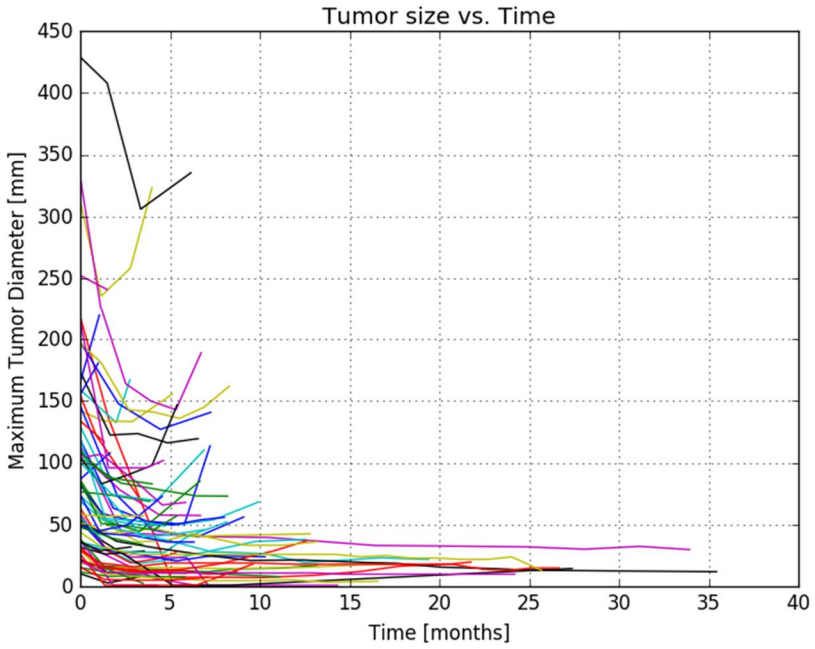

Figure 1. Maximum Tumor Diameter [mm] vs. Time [months].

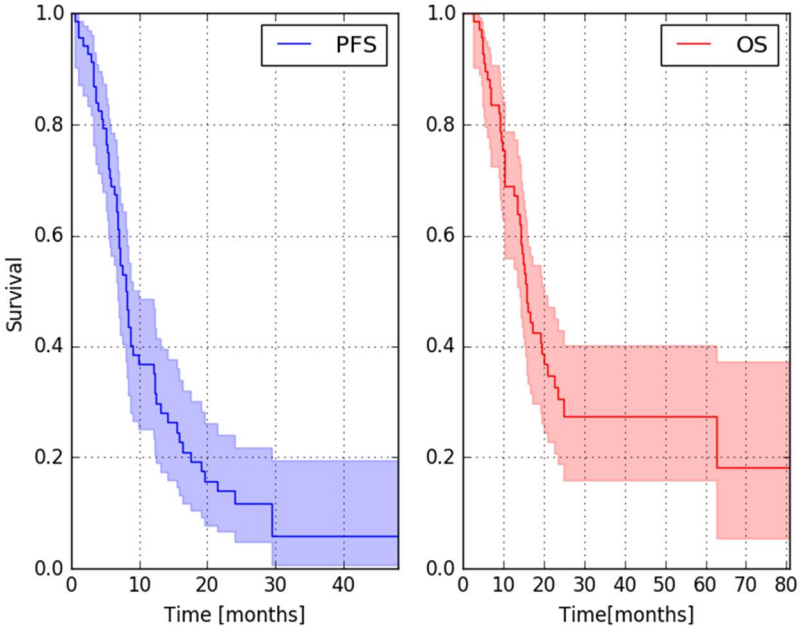

Figure 2. Kaplan Meier Curves of Progression Free (left) and Overall (right) Survival.

3. Exploratory Data Analysis

Definitions.

- Early tumor shrinkage (ETS): A reduction of at least 20% in tumor size at first reassessment
- Depth of response (DoR): The maximal tumor shrinkage observed in a patient
- Early shrinkage rate (Ksh): Relative reduction in tumor size at first reassessment calculated as [log (tumor size at first visit) – log (baseline tumor size)]/visit interval

Scatterplots were generated to spot possible correlations among the above variables. Regression analysis was performed to characterize the correlation quantitatively.

Simple linear regression analyses of log(PFS) were done to search for covariates affecting PFS. Semi-parametric Cox-PH analyses were then performed to assess factors affecting relative risks of PD events.

Baseline tumor size was regressed against other patient covariates to check for factors that positively correlate with it. This will be useful in cases where we do not have baseline tumor size measurement.

Finally, effect of trastuzumab treatment was assessed by calculating depth of response and median (and mean) PFS in treatment and non-treatment groups and was stratified by HER2 receptor status.

Analyses were performed using Python 2.7 and R.

4. MODELS

All model parameters were estimated using NONMEM software version 7.3. R (RStudio) and Python 2.7 were used for additional data exploration, analysis, and simulations.

A. Tumor Size Model

Two types of cancer cells – those sensitive to at least one of the drugs used and those resistant to all drugs – were assumed in our model. In line with Norton-Simon hypothesis,[6] specific growth rate (SGR) was assumed to decrease with increasing tumor size.[37,38] Logistic growth model was used to capture this property.

In addition, increase of SGR with time was assumed to occur at a rate of β.

$$k_g(\mathrm{t}) = k_g(0) + \beta \cdot \mathrm{t} - \mathrm{Eff} \qquad (2.1.1)$$

Chemotherapy was assumed to trigger cell death with a time delay governed by the equilibrium rate constant of the virtual compartment. Since all patients were treated with cisplatin and 5-FU/capecitabine, there was no placebo group to estimate efficacies of these drugs. Hence, drug effects of these agents were lumped under an umbrella term of 'cytotoxic drug effect' that was assumed as being proportional to the sum of log(exposure) of each drug.

$$\text{Cytotoxic drug effect} = k_{eff,1} \cdot \{\log(Cisplatin) + \log(5 - FU)\} \qquad (2.1.2)$$

Since placebo group does exist for trastuzumab, its efficacy was separately estimated as a model parameter. There is evidence that trastuzumab and cisplatin show synergistic effects.[39] Hence, it must be understood that the term 'trastuzumab drug effect' is a drug effect of trastuzumab conditioned on concurrent chemotherapy

of cisplatin.

$$\text{Trastuzumab drug effect} = k_{eff,2} \cdot \log(Trastuzumab) \quad (2.1.3)$$

In drug resistant tumor cells, Eff = 0, in which case the following is true.

$$k_g(t) = k_g(0) + \beta \cdot t \quad (2.1.4)$$

Henceforth, we will denote $k_g(t)$ of sensitive and resistant tumor cells as $k_{g,s}(t)$ and $k_{g,r}(t)$, respectively.

The parameter $k_g(0)$ is generally difficult to estimate since pre-treatment tumor sizes (based on RECIST evaluation) are often unavailable. The only pre-treatment information given is the baseline tumor size N(0). Since higher $k_g(0)$ would have given rise to higher N(0), a plausible guess would be that $k_g(0)$ is roughly proportional to log(N(0)). Hence, the following linear model was used to estimate $k_g(0)$.

$$k_g(0) = k_g(0)\_\text{intercept} + k_g(0)\_\text{slope} \cdot \log(N(0))$$

KPD model [34] was used to describe the time course of drug exposure.

$$\dot{C} = \delta - k_{DE} \cdot C \quad (2.1.5)$$

$$\dot{E} = k_{DE} \cdot C - k_{DE} \cdot E \quad (2.1.6)$$

In the above equation, *E* represents hypothetical drug amount in the effect site. A first-order elimination of *E* was assumed. δ stands for dirac delta function that represents drug input given as a bolus. Percent standard doses of trastuzumab, cisplatin, and capecitabine were used as input doses.

Denoting sensitive and resistant tumor cells as S and R, their rate of change can be described as:

$$\dot{S} = k_{g,s} \cdot S \cdot (1 - \frac{N}{N_{max}}) \quad (2.1.7)$$

$$\dot{R} = k_{g,r} \cdot R \cdot (1 - \frac{N}{N_{max}}) \quad (2.1.8)$$

$$N = S + R \quad (2.1.9)$$

$$S(0) = Fr \cdot N(0) \quad (2.1.10)$$

$$R(0) = (1 - Fr) \cdot N(0) \quad (2.1.11)$$

N represents total tumor size and N_{max} maximum tumor size.

N(0), S(0), and R(0) represent the initial size of total, sensitive, and resistant tumor cells. Fr is a parameter that represents the fraction of N(0) that is sensitive to cytotoxic effects. In the actual modeling, Fr has been subdivided into 7 fractions, each representing a specific combination of chemotherapeutic regimen ($=_3C_1 + {}_3C_2 + {}_3C_3$).

To estimate Fr, we have introduced two parameters P and Q. P represents the probability of resistance to cytotoxic agents (cisplatin and 5-FU/capecitabiine). Q represents the probability of resistance to trastuzumab. P and Q were assumed independent of each other.

To constrain P and Q within the interval of [0, 1], separate parameters ζ and κ were introduced such that $P = \frac{\zeta}{1+\zeta}$ and $Q = \frac{\kappa}{1+\kappa}$.

Fr was then calculated as follows:

$$Fr = P^2(1 - Q) + 2(1\text{-}P)PQ + 2P(1\text{-}P)(1\text{-}Q) + (1 - P)^2(1 - Q)$$

In Eq. (2.1.7) and (2.1.8), N_{max} was assumed to be proportional to Log(N(t=0)) to reflect the characteristics of nutrient-limited tumor growth.[40] The density dependence term (1 - $\frac{N}{N_{max}}$) reflects the assumption proposed by Norton-Simon hypothesis.[10]

The schematic diagram describing the final tumor size model is shown in Figure 3.

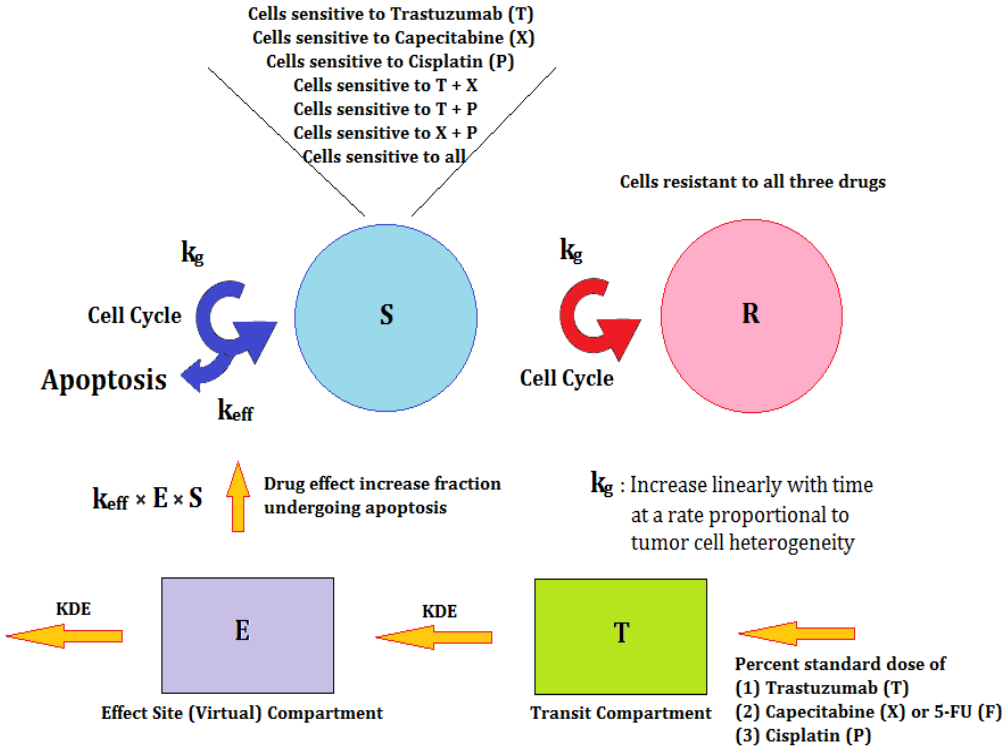

Figure 3. Diagram of treatment response model.

The meaning of the model parameters are explained based on a typical tumor growth curve. (See Figure 4)

1) The initial slope of tumor shrinkage is closely represented by $k_g(0)$ - k_{eff}.

2) Depth of response (DoR) is maximum percentage tumor shrinkage.[41] Based on our model, DoR is strongly determined by total fraction of sensitive clones, k_{eff}, and β.

3) Length of stable disease (SD) – defined as a state of neither sufficient shrinkage to qualify for PR nor sufficient increase to qualify for PD [42] – depends on the magnitude of β. If β = 0, no resistance would develop and tumor size would reach an asymptote.

4) The slope of the regrowth phase is primarily determined by β.

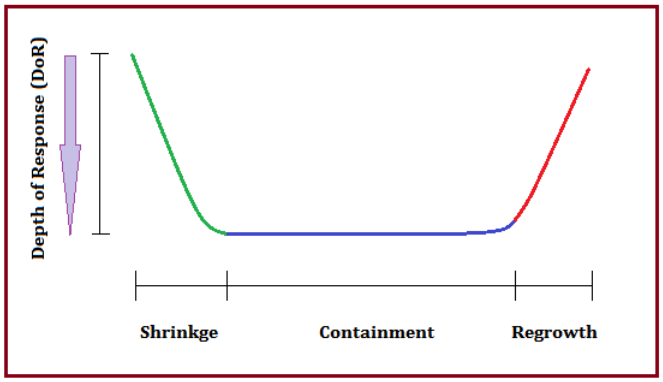

Figure 4. A typical tumor curve under treatment.

B. Covariate Model

Candidate covariates are demographic factors (such as age, weight, and gender) and clinical characteristics such as ECOG score, WHO histologic grade, HER2 receptor positivity, location of primary tumor, and types and number of metastatic organs.

Covariate search was done based on clinically known or suspected relationships and EBEs vs. covariate plots. Candidate covariates were then tested using stepwise covariate model building.[43]

C. Survival Model

(A) PFS prediction model

Two versions of PFS, which we denote as PFS1 and PFS2, were estimated.

PFS1 was simply calculated from the tumor size model because the model yields the full growth curve. For PFS2, a separate time-to-event model to predict PD based on non-measurable lesion was constructed. Henceforth, we will denote the model used for generating PFS1 and PFS2 as Model 1 and 2, respectively.

PFS prediction was obtained by selecting the smaller of the two estimates as below.

$$\text{PFS} = \min(PFS_1,\ PFS_2)$$

A probability distribution of patient dropouts was also estimated and was used to generate censored events. Different parametric distributions – exponential, Weibull, log-logistic, and Gompertz – were fitted to time-to-event data.

(B) PPS prediction model

Post-progression survival (PPS) is defined as the difference of overall survival (OS) and progression free survival (PFS). PPS should depend partly on the clinical outcome of first-line chemotherapy, but also on subsequent treatment.

Cox-proportional hazards regression [44,45] was conducted to assess the significance of the candidate covariates. Using the selected covariates, parametric survival model assuming different hazard functions (exponential, Weibull, and log-logistic) were constructed. The model yielding the lowest objective function value was selected as the final PPS prediction model.

D. Model Evaluation

Model fit was first assessed using basic goodness of fit plots. Then, model evaluation was done based on objective function values (OFVs) and estimated standard errors of model parameters. The final model was evaluated using a visual predictive check (VPC) of tumor size observations and posterior predictive checks using DoR, PFS, and PPS.

Relative bias and relative squared error were calculated, as defined below, for training and test datasets, where Obs denotes the observed value in test dataset and Pred denotes the predicted Obs value obtained using the final model.

$$\text{Relative error (\%)} = \frac{Obs-Pred}{Pred} \times 100$$

$$\text{Squared error} = (Obs - Pred)^2$$

$$\text{Relative squared error} = \left(\frac{Obs-Pred}{Pred}\right)^2 \times 100$$

Since dosing information was not available for the validation dataset, the standard dosing scheme that was used for the index dataset was assumed. Dosing interval was set to 3 weeks (=0.75 month). Full standard doses were given.

III. RESULTS

1. Exploratory Data Analysis

A. Baseline tumor size, Ksh, and DoR

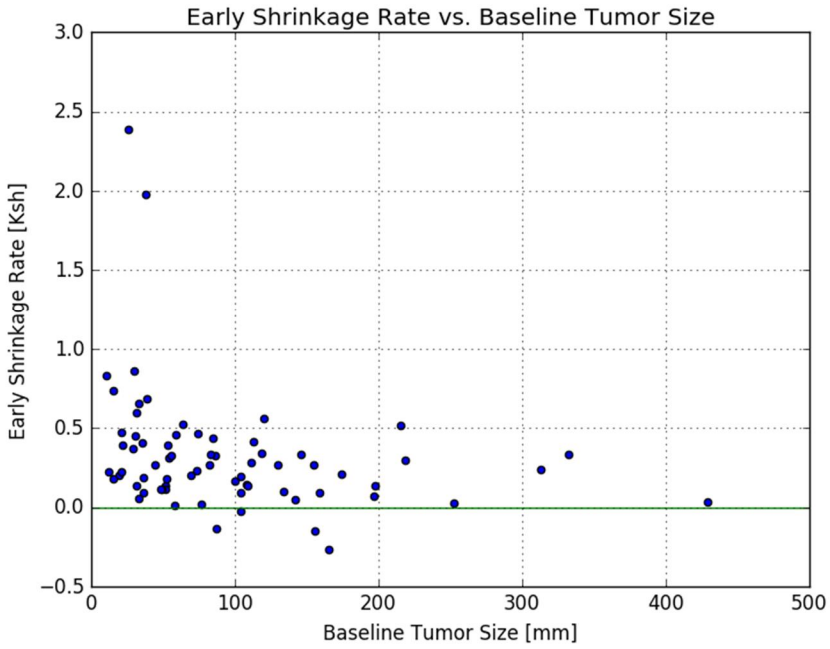

Figure 5. Baseline tumor size [mm] vs. early tumor shrinkage rate [/mo].

In figure 5, larger baseline tumor size is associated with lower Ksh.

A simple linear regression was carried out. Since linear regression is sensitive to outliers, two patients with Ksh greater than 1.5 were excluded.

The fitted regression equation is as follows (R^2=0.16) :

$$Ksh = 0.62 - 0.10 \log(baseline) \text{ (HER2 = 0, 1+, 2+)} \quad \ldots (3.1.1)$$

$$Ksh = 0.73 - 0.10 \log(baseline) \text{ (HER2 = 3+)} \quad \ldots (3.1.2)$$

The higher intercept of the regression equation in HER2 3+ patients suggests faster initial tumor shrinkage in these patients.

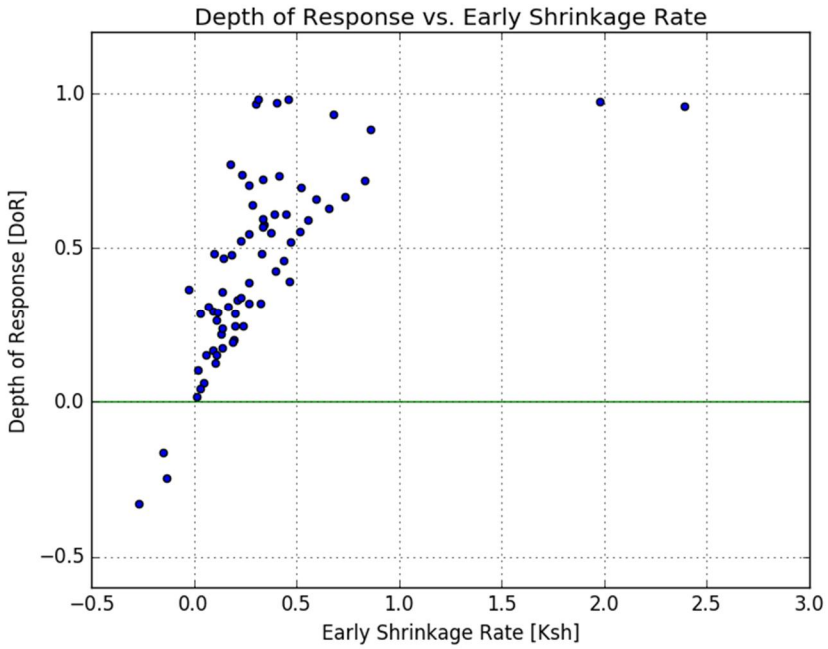

Figure 6. Depth of response (DoR) vs. Early shrinkage rate.

With known Ksh, we can predict DoR by fitting the following nonlinear equation to the observations.

$$\text{DoR} = \frac{K_{sh}}{\theta + K_{sh}} \quad \ldots (3.1.3)$$

Inspecting Eq. (3.1.3), DoR approaches 1 as Ksh goes to infinity. The parameter θ is equal to the magnitude of Ksh that results in DoR of 50%. Fitting our data using

non-linear least squares resulted in the estimate of θ = 0.51. Taking a step further, covariate model building was carried out.

$$\text{DoR} = \frac{K_{sh}}{\theta \exp(Covariate) + K_{sh}} \quad \ldots (3.1.4)$$

The only significant covariate was found to be HER2 3+ status.

The resultant regression equation is as follows:

$$\text{DoR} = \frac{K_{sh}}{0.41 \exp(-0.56\ (HER2{=}3+)) + K_{sh}} \quad \ldots (3.1.5)$$

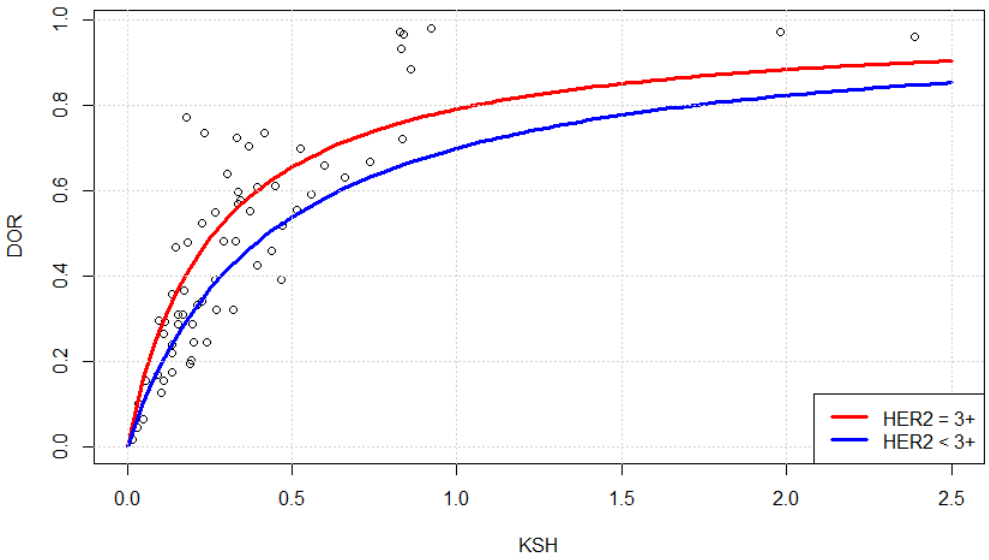

Figure 7. Predicted DoR vs. Ksh in HER2 3+ and 0/1+/2+ patients.

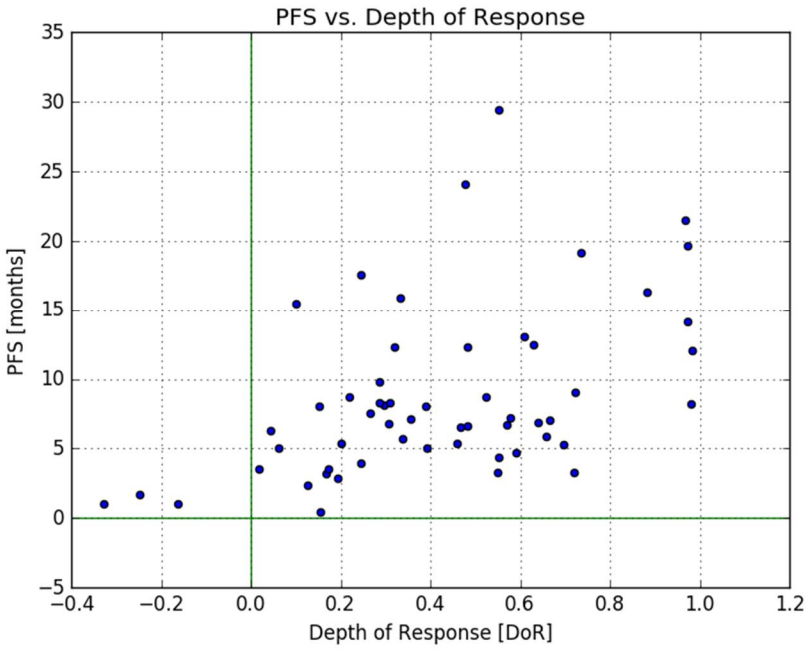

Figure 8. PFS as a function of DoR.

Performing a simple linear regression of log(PFS) using DoR as a predictor variable yields the following equation (adjusted R^2=0.36) :

$$\text{Log(PFS)} = 1.13 + 1.51\ \text{DoR} \qquad \ldots (3.1.6)$$

DoR alone explains about 36% of the total variability in PFS ($p = 6.38 * 10^{-7}$).

The remaining unexplained variability of 64% is likely related to non-measurable lesions. In our data, 30.43% of the patients were diagnosed PD based on non-measurable lesions.

Since DoR can only be known with certainty after PD as occurred, Eq. (3.1.6) has very little predictive value. It should be checked whether predicted DoR using Ksh based on Eq. (3.1.5) yield similar results. Since Ksh can be assessed at the first

patient visit, PFS can be predicted by using DoR predicted using Ksh. Following equation shows the regression result (adjusted R^2=0.22).

$$\text{Log(PFS)} = 1.07 + 1.58\ \text{DoR} \quad \ldots (3.1.7)$$

The p-value of DoR is 0.000142. The coefficient of determination R^2 decreased from 0.36 to 0.22.

Using predicted Ksh based on Eq. (3.1.1) and (3.1.2), DoR can be predicted using Eq. (3.1.5). Obviously, the predicted DoR now consists of uncertainties emanating from both Ksh prediction from baseline and DoR prediction from Ksh (adjusted R^2=0.13).

$$\text{Log(PFS)} = 1.33 + 1.25\ \text{DoR} - 0.38\ \text{Liver} \quad \ldots (3.1.8)$$

The uncertainty introduced by using predicted Ksh to predict DoR is partly compensated by using the information of liver metastasis. Whichever version of DoR is used, the estimates of the DoR coefficient are quite similar. The p-values of DoR and liver metastasis are 0.0287 and 0.0485, respectively and adjusted R^2 is now 0.13. 87% of the variability in PFS remains unexplained.

The results of Cox-proportional hazard models are discussed.

Using observed DoR, logrank test resulted in p value of 5.71e-07. The relative risk of PD decreases by 3% with each 1% increase in DoR. The p-value of the estimated coefficient if 1.01e-06.

Covariate model building resulted in ECOG score, liver metastasis, and signet-ring cell histology being selected.

Table 2. Significant covariates affecting PFS using observed DoR

Covariates	Relative risk	Significance (p-value)
Depth of response	0.96 (per 1% increase)	2.03e-08 ***
ECOG=2	6.58 (relative to ECOG=0)	0.0004 ***
ECOG=3	10.18 (relative to ECOG=0)	0.047 *
Histologic grade =4 (Signet ring cell type)	12.10 (relative to well-differentiated histologic type)	0.0025 **
Liver metastasis	2.34	0.015 *
Age	1.03 (per 1 year increase)	0.045 *

Signif. codes: 0 '***' 0.001 '**' 0.01 '*' 0.05

Each 1% increase in DoR was associated with 3.8% decrease in relative risk. Relative to ECOG score of 0, ECOG=1 was associated with increase in relative risk by 83% (p=0.064), ECOG=2 by 557.73% (p=0.0004), and ECOG=3 by 917.67% (p=0.047). Signet ring cell histology increased relative risk by 1110.06% relative to well-differentiated histologic type (p=0.0025). Presence of liver metastasis resulted in increase of relative risk by 134.48% (p=0.015). Increase of age by 1 year resulted in an increased relative risk by 3.02%. The logrank test resulted in p value of 4.352e-08.

Table 3. Significant covariates affecting PFS using predicted DoR using observed Ksh

Covariates	Relative risk	Significance (p-value)
Depth of response (predicted)	0.97 (per 1% increase)	0.00041 ***
ECOG=1	1.97 (relative to ECOG=0)	0.037 *
ECOG=2	3.85 (relative to ECOG=0)	0.0087 **
Histologic grade =4 (Signet ring cell type)	6.18 (relative to well-differentiated histologic type)	0.02 *
Liver metastasis	2.15	0.02 *

Signif. codes: 0 '***' 0.001 '**' 0.01 '*' 0.05

Age was not a significant covariate when predicted DoR was used.

In all cases, DoR seem to be a significant predictor of PFS. If we could increase DoR by 1%, we can theoretically reduce risk of PD by about 3%.

Shown below is a table of correlation coefficients of baseline tumor size (i.e. target lesion sum) with metastatic organs.

Table 4. Metastatic status and baseline tumor size

Organ involved	Correlation coefficient with baseline
Liver (solid organ)	0.24
Lung (solid organ)	0.26
Ovary (solid organ)	0.25
Distant lymph nodes	-0.011

Peritoneum (unmeasurable)	-0.022
Bone infiltration (unmeasurable)	0.026

Assessment of trastuzumab effect stratified by HER2 receptor status is shown in the following table.

Table 5. Response rate (RR), depth of response (DOR) and PFS stratified by trastuzumab treatment and HER2 receptor status

		HER2 0/1+/2+	**HER2 3+**
No Trastuzumab	RR	25% (1/4)	57.14% (4/7)
	DOR	26.12% ± 20.73%	40.75% ± 19.10%
	PFS	225 days (median) 197 days (mean)	151 days (median) 141 days (mean)
Trastuzumab	RR	50% (8/16)	78.57% (33/42)
	DOR	29.02% ± 19.18%	54.88% ± 28.34%
	PFS	153 days (median) 184 days (mean)	246 days (median) 314 days (mean)

Interestingly, RR and DOR were higher in HER2 3+ patients compared to HER2 0/1+/2+ patients in the no trastuzumab group despite shorter PFS. However, this difference was not statistically significant.

B. Distribution of DoR

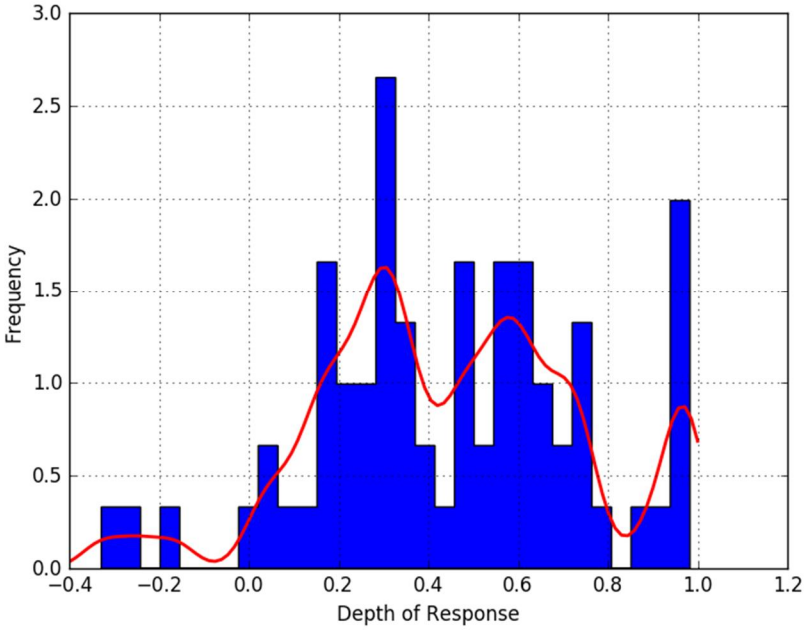

Figure 9. Histogram with kernel density estimates of DoR overlaid.

Figure 9 shows the empirical distribution of observed DoR in our data. There is suggestion of multi-modality in the distribution.

Based on the above, DoR was clustered into four groups – 1: non-responder, 2: partial responder (low), 3: partial responder (high), and 4: complete responder. Division into these four clusters was implemented using K-means clustering algorithm.

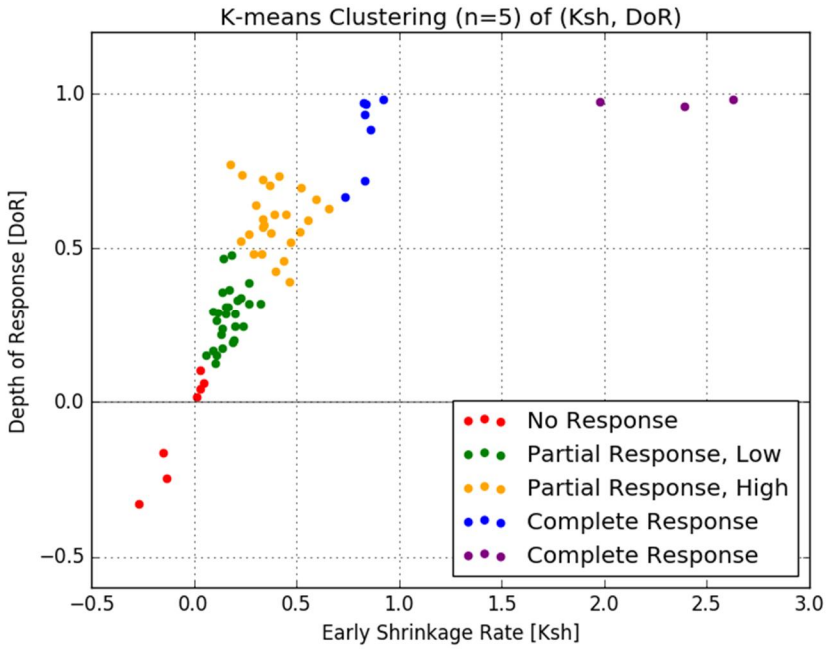

Figure 10. K-means clustering of (Ksh, DoR).

Decision tree classification was performed using R package *'rpart'* to identify predictors of the above clusters. (1: Complete Response, 2: Partial Response (High), 3: Partial Response (Low), 4: No Response)

The final tree after pruning resulted in the following:

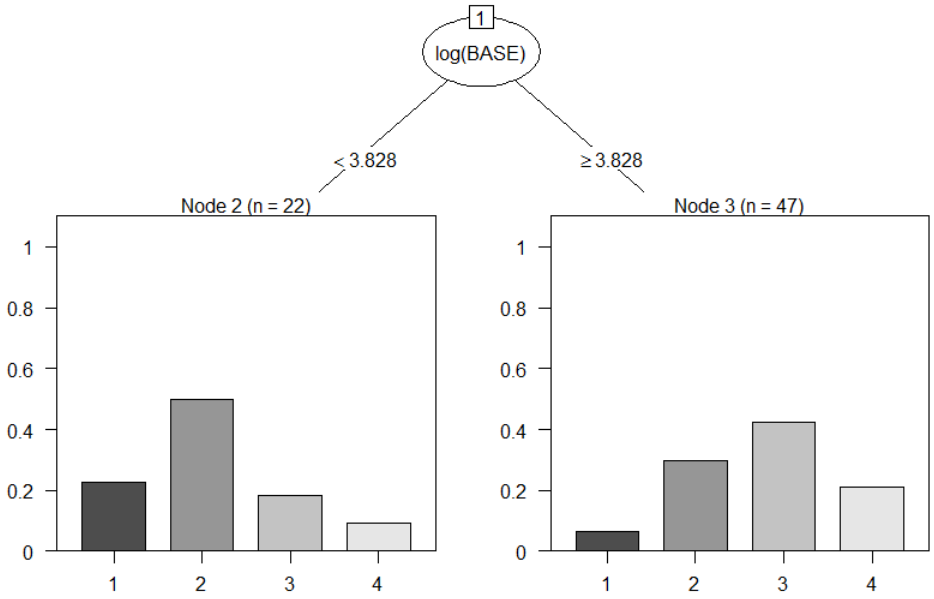

Figure 11. Pruned decision tree diagram to predict DoR class.

The only significant factor determining the response is log(baseline). The resultant probability masses of Node 2 and 3 are nearly mirror images of each other.

2. Tumor Size Model

The parameter estimates of the final tumor size model are summarized in Table 6.

Table 6. Estimation result of tumor size model

Parameter	Estimate	RSE (%)

Coefficient of drug efficacy (k_{eff})		
Cytotoxic drugs + Immune surveillance	17.29	32.18
Trastuzumab	1.78	18.32
Rate of tumor progression (β)		
Well differentiated	0	-
Moderately differentiated	0.084^2	33.55
Poorly differentiated	0.15^2	25.78
Signet ring cell	0.37^2	17.99
Fraction of tumor cells resistant to		
Cisplatin/Capecitabine/5-FU ζ (P)	8.50 (0.89)	27.67
Trastuzumab κ (Q)		
HER2-H	1.59 (0.61)	24.53
HER2-L	2.27 (0.69)	42.89
KDE (/month)	0.81	27.22
Maximum tumor size (N_{max}) (mm)	71.46·log(base)	0.17
Intercept of initial SGR	-0.14	9.27
Slope of initial SGR		
HER2-H	0.03	13.32
HER2-L	0.051	20.73
Inter-individual Variability		

$\omega_{slope\_initial\ SGR}$(CV%)	64.64	15.04
ω_{β}(CV%)	119.2	21.44
$\omega_{\zeta,\kappa}$ (CV%)	158.8	13.27
Residual error		
$\sigma_{Additive}$	2.62	12.96

(k_{eff}: Cell kill coefficient, β: Coefficient of tumor progression rate, N_{max}: Maximum tumor size)

HER2 3+ status was associated with larger spread of trastuzumab and cisplatin/5-FU resistance probabilities.

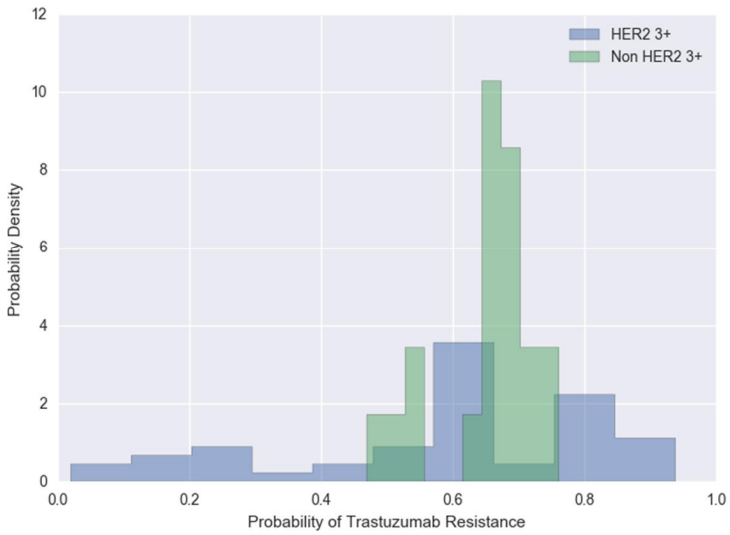

Figure 12. Distribution of post-hoc trastuzumab resistance probability.

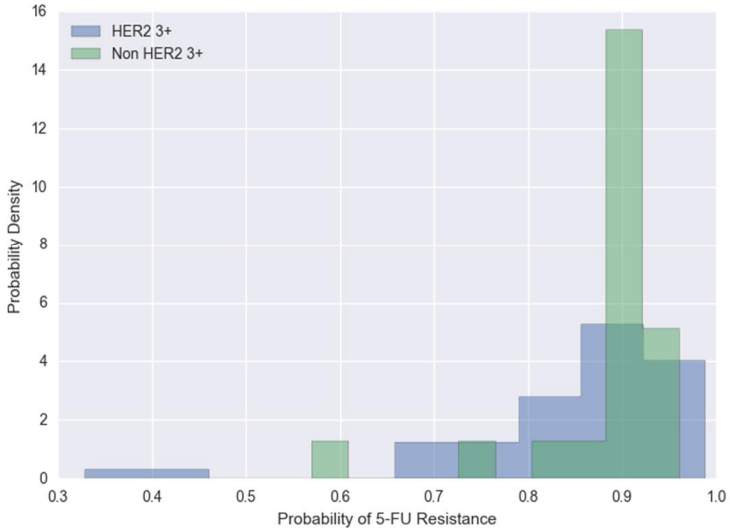

Figure 13. Distribution of post-hoc 5-FU resistance (=cisplatin resistance) probability.

3. Survival Model

A. PFS prediction model

Log-logistic hazard model provided the best fit to describing the hazard of appearance of new lesion or progression of target lesions. The estimate of this hazard was 0.099/month. Prior gastrectomy history and ECOG score were found as significant covariates.

Following is a table showing the estimation result of the Model 2.

Table 7. Estimation results of Model 2

Covariate	Estimate (RSE%)	Relative Risk (p-value)
PFS based on non-measurable lesions		
Baseline hazard (mo^{-1})	0.099 (27.98)	-
Shape parameter	2.07 (25.23)	-
Prior gastrectomy	-1.89 (23.6)	0.15 (0.00013)
ECOG score	0.87 (38.46)	0.87 (0.014)

B. PPS prediction model

PFS was found to be a significant predictor of PPS when histologic grade is well- or moderately differentiated. Age was marginally significant.

Log-logistic hazard model seemed to best fit our data. Predicted PFS of Eq. (3.1.8) was used as a covariate. When histologic grade is either poorly differentiated or signet ring cell, it seems that PFS has no effect on patient outcome. When histologic grade is either well- or moderately differentiated, longer PFS and smaller baseline tumor size are associated with a lower hazard.

Table 8. Estimation results of PPS prediction model

Covariate	Estimate (RSE%)	Relative Risk (p-value)
Post-progression survival model		
Baseline hazard (mo^{-1})	0.17 (22.98)	-
Shape parameter	0.78 (30.55)	-
Length of PFS (month)	-0.0623 (41.87)	0.94 (0.0066)
Tumor size at last assessment (1 SD[a])	0.35 (32.87)	1.42 (0.038)

[a] standard deviation

4. Model Evaluation

A. Goodness of fit plots of the tumor size model

Following is a mirror plot showing observed and predicted tumor sizes.

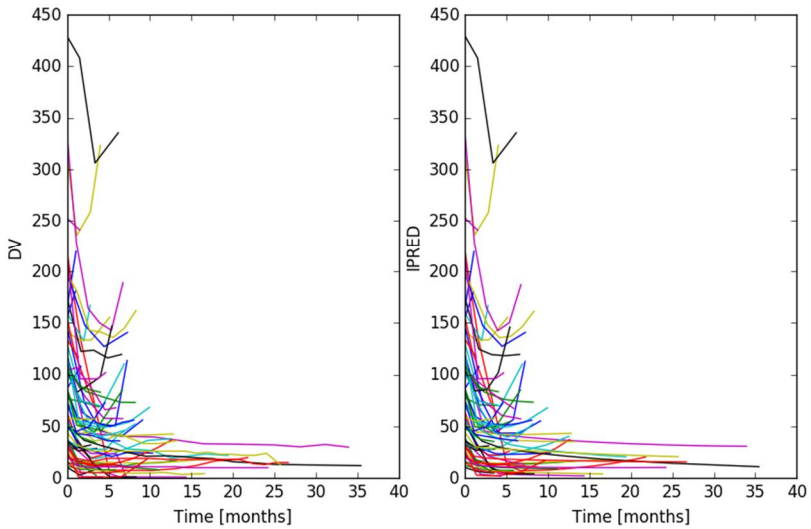

Figure 14. Mirror plots of the tumor size model.

The tumor size model seems sufficiently flexible to fit the observed tumor sizes with appropriate choice of random effects. Following are goodness of fit plots.

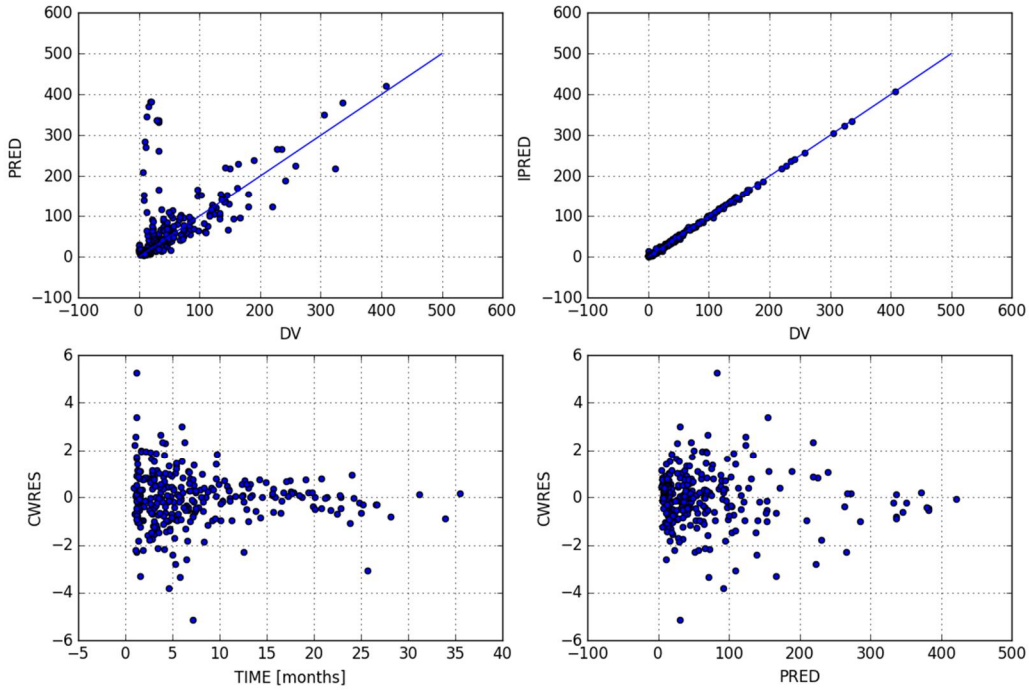

Figure 15. Basic goodness of fit plots of the tumor size model.

B. Validation

Following are VPCs of tumor size model generated on index and validation datasets, respectively.

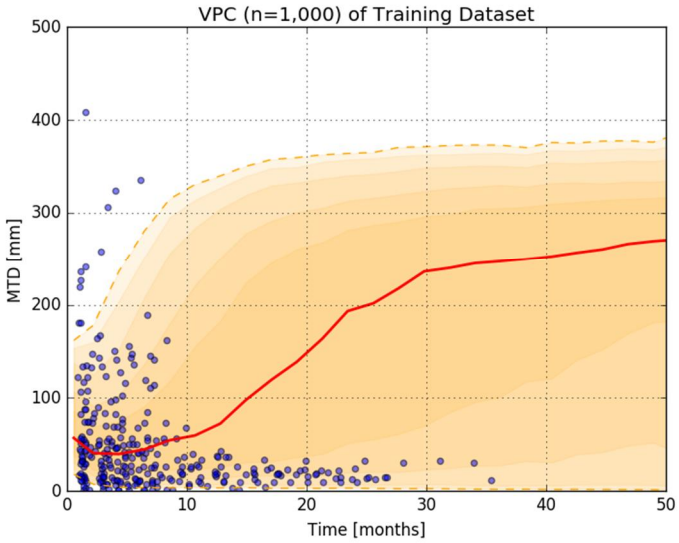

Figure 16. VPC of the tumor size model using the index dataset (n=1,000).

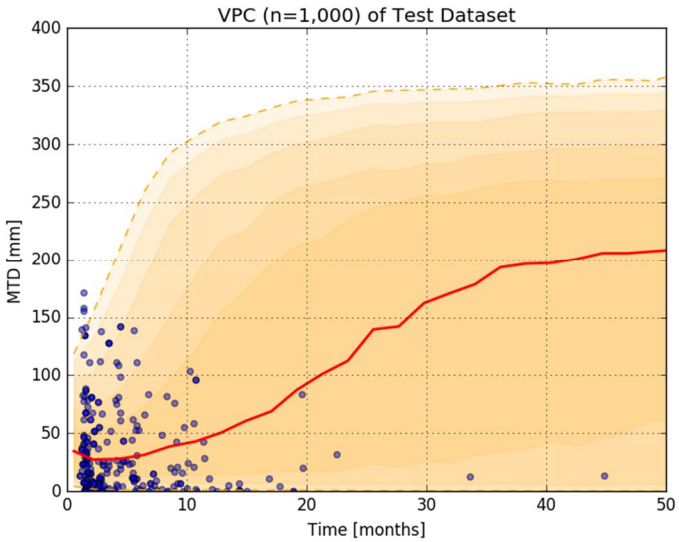

Figure 17. VPC of the tumor size model using the validation dataset (n=1,000).

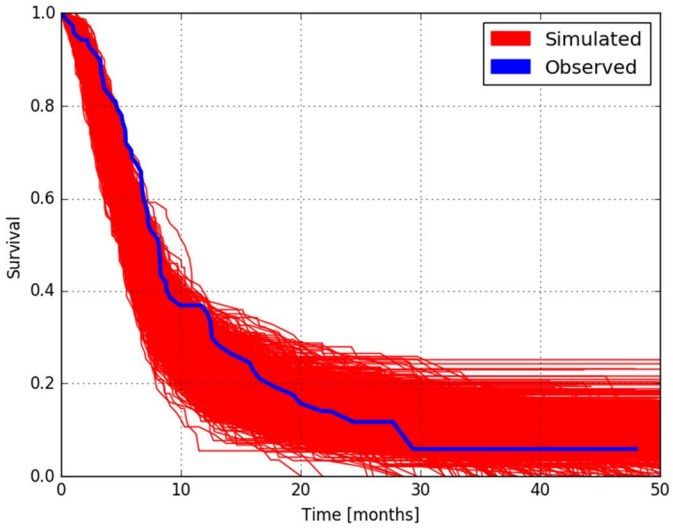

Figure 18. Simulated (red) and observed (blue) KM survival curves of PFS using training data (n=1,000).

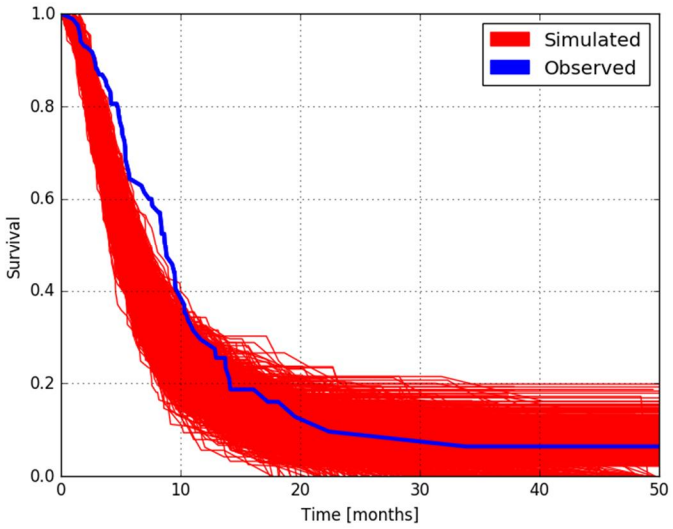

Figure 19. Validation of PFS prediction using test data (n=1,000)

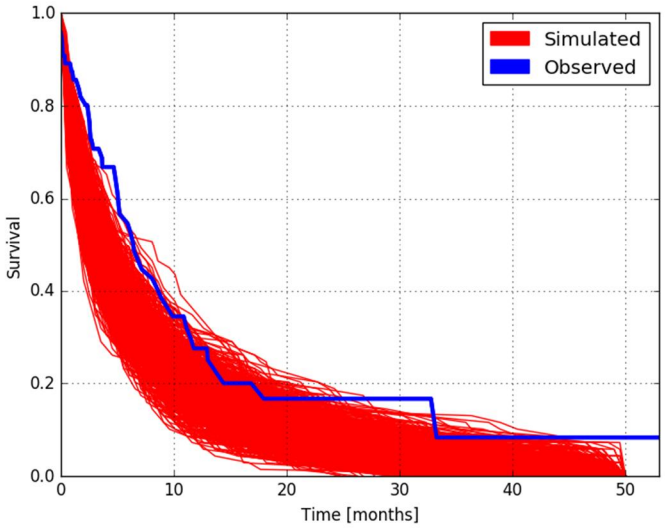

Figure 20. Simulated (red) and observed (blue) KM survival curves of PPS using training data (n=1,000).

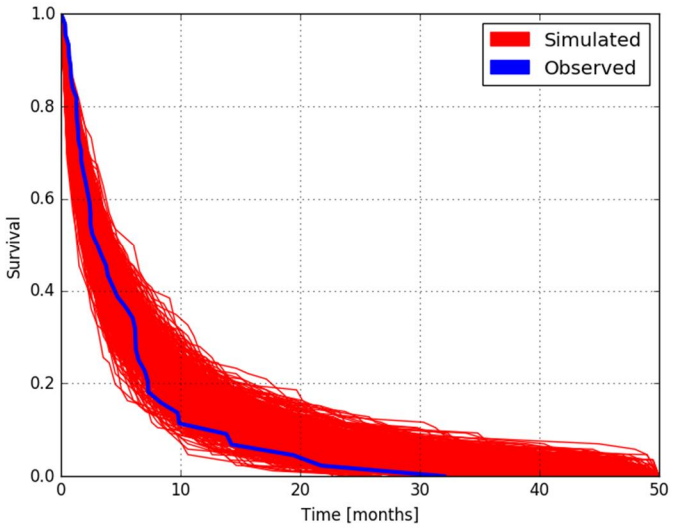

Figure 21. Validation of PPS prediction using test data (n=1,000).

Kaplan Meier survival curves were overlaid with the observed survival curve of the index and validation datasets.

Censoring distribution was used to generate censored time events. The simulated curves coincide well with the observed curves, although there is a slight tendency to underestimate PFS in the early period (<10 months).

In conclusion, our models seem to generalize well to unseen data in terms of predicting PFS and PPS.

IV. DISCUSSION

1. Data

There are significant differences of baseline SLD, HER2 receptor status, and proportions of patients with previous gastrectomy between training and test datasets (see Table 1).

The main cause of the difference in SLD between the two datasets is likely due to using different versions of RECIST in assessing sum of tumor diameters of the target lesion[46]. RECIST 1.0 was used for the training dataset while RECIST 1.1 was used for the test dataset, which was prepared in the final stage of analysis.

As for the difference in the proportions of HER2 receptor status, this is a result of deliberately enriching the test dataset with HER2 negative patients to see whether the model generalizes well to these patients.

2. Tumor size model (Model 1)

Key findings based on the estimation results of Model 1 are as follows.

1) HER2 receptor status is crucial in predicting response to trastuzumab. Our results suggest that higher HER2 receptor density is associated with lower probability of trastuzumab resistance.

2) Higher histologic grade is associated with faster tumor progression.

3) Larger tumor is associated with faster tumor progression.

Model validation using visual predictive check and relative bias estimates suggest that our model generates reliable predictions for external, unforeseen observations.

3. Survival Model

A. PFS prediction model

1) PFS prediction model

Risk factors that lead to higher probability of non-target lesion progression - ECOG score and previous gastrectomy status - were successfully identified. Baseline hazard was best described using log-logistic distribution and suggests that the hazard initially increases and then decreases.

The cause of prior gastrectomy being associated with a lower probability of non-target lesion progression is unclear. It is possible that this is due to lower trastuzumab clearance in patients with prior gastrectomy [14].

B. PPS prediction model

The estimated parameters shown in Table 3 suggest the following:

(1) Mortality is greatest immediately after PD diagnosis and decreases thereafter.

(2) Longer PFS and smaller tumor size at last assessment are associated with a survival benefit when WHO histologic grade is I or II (i.e. well-differentiated or moderately differentiated). With higher histologic grades, survival does not seem to be affected by these factors.

V. CONCLUSION

This work successfully characterized dose-response relationship and important covariates affecting treatment response under the KPD modeling framework. The developed model was successfully validated using an out-of-sample dataset. Based on the model, it is possible to generate individualized predictions of treatment response and patient survival. This will help optimize treatment in HER2 positive metastatic gastric cancer patients.

REFERENCES

1 Bang, Y. J., Van Cutsem, E., Feyereislova, A., Chung, H. C., Shen, L., Sawaki, A. *et al.* Trastuzumab in combination with chemotherapy versus chemotherapy alone for treatment of HER2-positive advanced gastric or gastro-oesophageal junction cancer (ToGA): a phase 3, open-label, randomised controlled trial. *Lancet* **376**, 687-697, doi:10.1016/S0140-6736(10)61121-X (2010).

2 Shitara, K., Yatabe, Y., Matsuo, K., Sugano, M., Kondo, C., Takahari, D. *et al.* Prognosis of patients with advanced gastric cancer by HER2 status and trastuzumab treatment. *Gastric cancer : official journal of the International Gastric Cancer Association and the Japanese Gastric Cancer Association* **16**, 261-267, doi:10.1007/s10120-012-0179-9 (2013).

3 Luria, S. E. & Delbruck, M. Mutations of Bacteria from Virus Sensitivity to Virus Resistance. *Genetics* **28**, 491-511 (1943).

4 Norton, L., Simon, R., Brereton, H. D. & Bogden, A. E. Predicting the course of Gompertzian growth. *Nature* **264**, 542-545 (1976).

5 Goldie, J. H. & Coldman, A. J. The genetic origin of drug resistance in neoplasms: implications for systemic therapy. *Cancer research* **44**, 3643-3653 (1984).

6 Norton, L. & Simon, R. The Norton-Simon hypothesis revisited. *Cancer treatment reports* **70**, 163-169 (1986).

7 Swan, G. W. Cancer chemotherapy: optimal control using the Verhulst-Pearl equation. *Bulletin of mathematical biology* **48**, 381-404 (1986).

8 Frank, S. A. & Slatkin, M. Fisher's fundamental theorem of natural selection. *Trends in ecology & evolution* **7**, 92-95, doi:10.1016/0169-5347(92)90248-A (1992).

9 Lessard, S. Fisher's fundamental theorem of natural selection revisited. *Theoretical population biology* **52**, 119-136, doi:10.1006/tpbi.1997.1324 (1997).

10 Simon, R. & Norton, L. The Norton-Simon hypothesis: designing more

effective and less toxic chemotherapeutic regimens. *Nature clinical practice. Oncology* **3**, 406-407, doi:10.1038/ncponc0560 (2006).

11 Tham, L. S., Wang, L., Soo, R. A., Lee, S. C., Lee, H. S., Yong, W. P. *et al.* A pharmacodynamic model for the time course of tumor shrinkage by gemcitabine + carboplatin in non-small cell lung cancer patients. *Clinical cancer research : an official journal of the American Association for Cancer Research* **14**, 4213-4218, doi:10.1158/1078-0432.CCR-07-4754 (2008).

12 Claret, L., Girard, P., Hoff, P. M., Van Cutsem, E., Zuideveld, K. P., Jorga, K. *et al.* Model-based prediction of phase III overall survival in colorectal cancer on the basis of phase II tumor dynamics. *Journal of clinical oncology : official journal of the American Society of Clinical Oncology* **27**, 4103-4108, doi:10.1200/JCO.2008.21.0807 (2009).

13 Ribba, B., Kaloshi, G., Peyre, M., Ricard, D., Calvez, V., Tod, M. *et al.* A tumor growth inhibition model for low-grade glioma treated with chemotherapy or radiotherapy. *Clinical cancer research : an official journal of the American Association for Cancer Research* **18**, 5071-5080, doi:10.1158/1078-0432.CCR-12-0084 (2012).

14 Cosson, V. F., Ng, V. W., Lehle, M. & Lum, B. L. Population pharmacokinetics and exposure-response analyses of trastuzumab in patients with advanced gastric or gastroesophageal junction cancer. *Cancer chemotherapy and pharmacology* **73**, 737-747, doi:10.1007/s00280-014-2400-5 (2014).

15 Wang, Y., Sung, C., Dartois, C., Ramchandani, R., Booth, B. P., Rock, E. *et al.* Elucidation of relationship between tumor size and survival in non-small-cell lung cancer patients can aid early decision making in clinical drug development. *Clinical pharmacology and therapeutics* **86**, 167-174, doi:10.1038/clpt.2009.64 (2009).

16 Giessen, C., Laubender, R. P., Fischer von Weikersthal, L., Schalhorn, A., Modest, D. P., Stintzing, S. *et al.* Early tumor shrinkage in metastatic

colorectal cancer: retrospective analysis from an irinotecan-based randomized first-line trial. *Cancer science* **104**, 718-724, doi:10.1111/cas.12148 (2013).

17 Modest, D. P., Laubender, R. P., Stintzing, S., Giessen, C., Schulz, C., Haas, M. *et al.* Early tumor shrinkage in patients with metastatic colorectal cancer receiving first-line treatment with cetuximab combined with either CAPIRI or CAPOX: an analysis of the German AIO KRK 0104 trial. *Acta oncologica* **52**, 956-962, doi:10.3109/0284186X.2012.752580 (2013).

18 Piessevaux, H., Buyse, M., Schlichting, M., Van Cutsem, E., Bokemeyer, C., Heeger, S. *et al.* Use of early tumor shrinkage to predict long-term outcome in metastatic colorectal cancer treated with cetuximab. *Journal of clinical oncology : official journal of the American Society of Clinical Oncology* **31**, 3764-3775, doi:10.1200/JCO.2012.42.8532 (2013).

19 Cremolini, C., Loupakis, F., Antoniotti, C., Lonardi, S., Masi, G., Salvatore, L. *et al.* Early tumor shrinkage and depth of response predict long-term outcome in metastatic colorectal cancer patients treated with first-line chemotherapy plus bevacizumab: results from phase III TRIBE trial by the Gruppo Oncologico del Nord Ovest. *Annals of oncology : official journal of the European Society for Medical Oncology* **26**, 1188-1194, doi:10.1093/annonc/mdv112 (2015).

20 Miyake, H., Harada, K., Ozono, S. & Fujisawa, M. Prognostic Significance of Early Tumor Shrinkage Under Second-Line Targeted Therapy for Metastatic Renal Cell Carcinoma: A Retrospective Multi-Institutional Study in Japan. *Molecular diagnosis & therapy* **20**, 385-392, doi:10.1007/s40291-016-0206-3 (2016).

21 Miyake, H., Miyazaki, A., Imai, S., Harada, K. & Fujisawa, M. Early Tumor Shrinkage Under Treatment with First-line Tyrosine Kinase Inhibitors as a Predictor of Overall Survival in Patients with Metastatic Renal Cell Carcinoma: a Retrospective Multi-Institutional Study in Japan. *Targeted oncology* **11**, 175-182, doi:10.1007/s11523-015-0385-6 (2016).

22 Tsuji, A., Sunakawa, Y., Ichikawa, W., Nakamura, M., Kochi, M., Denda, T. *et al.* Early Tumor Shrinkage and Depth of Response as Predictors of Favorable Treatment Outcomes in Patients with Metastatic Colorectal Cancer Treated with FOLFOX Plus Cetuximab (JACCRO CC-05). *Targeted oncology*, doi:10.1007/s11523-016-0445-6 (2016).

23 Nishino, M., Jagannathan, J. P., Ramaiya, N. H. & Van den Abbeele, A. D. Revised RECIST guideline version 1.1: What oncologists want to know and what radiologists need to know. *AJR. American journal of roentgenology* **195**, 281-289, doi:10.2214/AJR.09.4110 (2010).

24 Mehrara, E., Forssell-Aronsson, E., Ahlman, H. & Bernhardt, P. Specific growth rate versus doubling time for quantitative characterization of tumor growth rate. *Cancer research* **67**, 3970-3975, doi:10.1158/0008-5472.CAN-06-3822 (2007).

25 de Aretxabala, X., Yonemura, Y., Sugiyama, K., Hirose, N., Kumaki, T., Fushida, S. *et al.* Gastric cancer heterogeneity. *Cancer* **63**, 791-798 (1989).

26 Yonemura, Y., Matsumoto, H., Ninomiya, I., Ohoyama, S., Kimura, H., de Aletxabala, X. *et al.* Heterogeneity of DNA ploidy in gastric cancer. *Analytical cellular pathology : the journal of the European Society for Analytical Cellular Pathology* **4**, 61-67 (1992).

27 Greaves, M. & Maley, C. C. Clonal evolution in cancer. *Nature* **481**, 306-313, doi:10.1038/nature10762 (2012).

28 Karev, G. P. & Kareva, I. G. Replicator Equations and Models of Biological Populations and Communities. *Math Model Nat Pheno* **9**, 68-95, doi:10.1051/mmnp/20149305 (2014).

29 Skipper, H. E. Kinetics of mammary tumor cell growth and implications for therapy. *Cancer* **28**, 1479-1499 (1971).

30 Skipper, H. E., Schabel, F. M., Jr. & Wilcox, W. S. Experimental evaluation of potential anticancer agents. XXI. Scheduling of arabinosylcytosine to take advantage of its S-phase specificity against leukemia cells. *Cancer chemotherapy reports. Part 1* **51**, 125-165 (1967).

31 Adams, D. J. In vitro pharmacodynamic assay for cancer drug development: application to crisnatol, a new DNA intercalator. *Cancer research* **49**, 6615-6620 (1989).

32 Norton, L. A Gompertzian model of human breast cancer growth. *Cancer research* **48**, 7067-7071 (1988).

33 Pillai, G., Gieschke, R., Goggin, T., Jacqmin, P., Schimmer, R. C. & Steimer, J. L. A semimechanistic and mechanistic population PK-PD model for biomarker response to ibandronate, a new bisphosphonate for the treatment of osteoporosis. *British journal of clinical pharmacology* **58**, 618-631, doi:10.1111/j.1365-2125.2004.02224.x (2004).

34 Jacqmin, P., Snoeck, E., van Schaick, E. A., Gieschke, R., Pillai, P., Steimer, J. L. *et al.* Modelling response time profiles in the absence of drug concentrations: definition and performance evaluation of the K-PD model. *Journal of pharmacokinetics and pharmacodynamics* **34**, 57-85, doi:10.1007/s10928-006-9035-z (2007).

35 Collett, D. Modelling Survival Data in Medical Research. *CRC Press, Taylor & Francis Group* **3e** (2015).

36 Xie, X., Strickler, H. D. & Xue, X. Additive hazard regression models: an application to the natural history of human papillomavirus. *Computational and mathematical methods in medicine* **2013**, 796270, doi:10.1155/2013/796270 (2013).

37 Lloyd, H. H. Estimation of tumor cell kill from Gompertz growth curves. *Cancer chemotherapy reports. Part 1* **59**, 267-277 (1975).

38 Bassukas, I. D. & Maurer-Schultze, B. The recursion formula of the Gompertz function: a simple method for the estimation and comparison of tumor growth curves. *Growth, development, and aging : GDA* **52**, 113-122 (1988).

39 Kim, S. Y., Kim, H. P., Kim, Y. J., Oh, D. Y., Im, S. A., Lee, D. *et al.* Trastuzumab inhibits the growth of human gastric cancer cell lines with HER2 amplification synergistically with cisplatin. *International journal of*

oncology **32**, 89-95 (2008).

40 Leadbeater, B. S. The 'Droop Equation'--Michael Droop and the legacy of the 'Cell-Quota Model' of phytoplankton growth. *Protist* **157**, 345-358, doi:10.1016/j.protis.2006.05.009 (2006).

41 Heinemann, V., Stintzing, S., Modest, D. P., Giessen-Jung, C., Michl, M. & Mansmann, U. R. Early tumour shrinkage (ETS) and depth of response (DpR) in the treatment of patients with metastatic colorectal cancer (mCRC). *European journal of cancer* **51**, 1927-1936, doi:10.1016/j.ejca.2015.06.116 (2015).

42 Eisenhauer, E. A., Therasse, P., Bogaerts, J., Schwartz, L. H., Sargent, D., Ford, R. *et al.* New response evaluation criteria in solid tumours: revised RECIST guideline (version 1.1). *European journal of cancer* **45**, 228-247, doi:10.1016/j.ejca.2008.10.026 (2009).

43 Wahlby, U., Jonsson, E. N. & Karlsson, M. O. Comparison of stepwise covariate model building strategies in population pharmacokinetic-pharmacodynamic analysis. *AAPS pharmSci* **4**, E27, doi:10.1208/ps040427 (2002).

44 Moghimi-Dehkordi, B., Safaee, A. & Tabei, S. Z. A comparison between Cox proportional hazard models and logistic regression on prognostic factors in gastric cancer. *East African journal of public health* **6 Suppl**, 20-22 (2009).

45 Liu, W., Hao, X. S., Fan, Q., Li, H. X., Song, L. N., Wang, S. J. *et al.* [Cox proportional hazard model analysis of prognosis in patients with carcinoma of esophagus and gastric cardia after radical resection]. *Zhonghua zhong liu za zhi [Chinese journal of oncology]* **30**, 921-925 (2008).

46 Jang, G. S., Kim, M. J., Ha, H. I., Kim, J. H., Kim, H. S., Ju, S. B. *et al.* Comparison of RECIST version 1.0 and 1.1 in assessment of tumor response by computed tomography in advanced gastric cancer. *Chinese journal of cancer research = Chung-kuo yen cheng yen chiu* **25**, 689-694,

doi:10.3978/j.issn.1000-9604.2013.11.09 (2013).

ABSTRACT (IN KOREAN)

HER2 양성 전이성 위암 환자의 Trastuzumab 치료반응 예측모델

<지도교수 박 경 수>

연세대학교 대학원 의과학과

채동우

목적

본 연구는 HER2 양성 전이성 위암 환자에서 포괄적 치료 반응 예측 모델을 수립하기 위하여 수행되었다.

방법

데이터는 세브란스 병원에서 수행된 ToGA 임상 시험에 참여한 69 명의 진행성 위암 환자로부터 얻어졌다. 각 방문 시마다 RECIST 평가가 이루어졌고 종양 크기는 최장축의 합(SLD)으로 측정하였다. 종양 크기 예측 모델, 비측정 병변의 PD 예측 모델, 그리고 PPS 예측 모델을 순차적으로 개발하여 환자의 치료 반응을 포괄적으로 기술하였다. 86 명의 환자로 이루어진 별도의 데이터를 이용하여 모델 검증을 수행하였다.

결과

개발된 TGI 모델에 의해 생성된 종양 크기 예측치는 관측치와 좋은 적합을 보였다. HER2 3+ 환자들이 HER2 1+/2+ 환자에 비하여 trastuzumab 에 대한 높은 감수성을 보였다. 높은 WHO 조직학적 등급은 빠른 종양 진행과 연관되었다. 위절제 수술 과거력과 낮은 ECOG 점수는 비측정 병변의 PD 에 대한 낮은 hazard 와 연관되었다. PFS 와 PPS 는 WHO 조직학적 등급이 I 또는 II 일 때 양성 상관을 보였다. 이러한 상관성은 WHO 조직학적 등급 III 과 IV 에서는 나타나지 않았다.

결론

개발된 모델에 근거하여 개인별 치료 반응과 생존을 예측하는 것이 가능할 것으로 생각된다. 이는 HER2 양성 전이성 위암 환자에서 치료를 최적화시키는데 도움이 될 것이다.